Sensors & Actuators: B. Chemical 377 (2023) 133122

Contents lists available at ScienceDirect

Sensors and Actuators: B. Chemical

journal homepage: www.elsevier.com/locate/snb

A molecular imaging tool for monitoring carboxylesterase 2 during early diagnosis of liver-related diseases

Jiaxin Li [a], Jingrui Cao [b], Wen Wu [b], Lanlan Xu [a], Siqi Zhang [a], Pinyi Ma [a,*], Qiong Wu [b,*], Daqian Song [a,*]

[a] College of Chemistry, Jilin Province Research Center for Engineering and Technology of Spectral Analytical Instruments, Jilin University, Qianjin Street 2699, Changchun 130012, China

[b] Key Laboratory of Pathobiology, Ministry of Education, Nanomedicine and Translational Research Center, China-Japan Union Hospital of Jilin University, 126 Sendai Street, Changchun 130033, Jilin, China

ARTICLE INFO

Keywords:
Carboxylesterase 2
Early diagnosis
Mitochondria-targeting
Ultra-high sensitivity
Bioimaging

ABSTRACT

Early disease diagnosis is crucial for human health and successful therapy. Carboxylesterase 2 (CES2), the main enzyme found in many tumor tissues, is closely associated with many malignant diseases. Therefore, the ability to detect endogenous CES2-associated diseases can be of therapeutic significance. In this study, we designed a novel mitochondria-targeting near-infrared (NIR) chemosensor (YDT) to visualize the endogenous CES2. This is the first study to track CES2 at the mitochondrial level and present the currently most sensitive CES2 detection sensor. With various features including large Stokes shift, quick response time, excellent selectivity, and ultra-high sensitivity, the sensor can overcome numerous limitations faced by traditional CES2 probes. YDT is an "off-on" chemosensor that releases fluorophore YD-1 upon interacting with CES2, emits strong fluorescence at 660 nm. Importantly, YDT can dynamically monitor immediate changes in CES2 level under external stimuli. Moreover, we used YDT to systematically study the CES2 expression in drug-induced liver injury and its remediation model, as well as in an inflammation model. With these outstanding characteristics, YDT is a considerably promising tool for further research on biological processes and for examining the physiological roles of CES2 in living systems.

1. Introduction

A variety of abnormally expressed enzymes are often used as biomarkers for monitoring cancers or other diseases, thus play an essential role in the early diagnosis of diseases, allowing for immediate assessment of human health [1,2]. Carboxylesterases (CES, E.C. 3.1.1.1) belong to the α/β-fold serine hydrolase family, which is a group of enzymes responsible for hydrolyzing various endogenous and exogenous substrates containing ester, amide, and thioester bonds, including fatty acid esters, environmental toxins, and ester-containing prodrugs [3–6]. Many types of cancer such as hepatocellular carcinoma, colon cancer, breast cancer, and pancreatic cancer, as well as malignant diseases such as obesity, atherosclerosis, and fatty liver disease, are tightly correlated with the abnormal expression of CES [7–10]. Furthermore, CES represent a multigene family that can be broadly classified into five isoforms according to their amino acid sequences [11–13]. As one of the vital phase I metabolic enzymes, carboxylesterase 2 (CES2) plays a critical role not only in the metabolism of endobiotics but also in the detoxification/activation of xenobiotics and metabolism of lipids [14,15]. Therefore, the development of a method to analyze CES2 in biological system is important for a better understanding of its biological functions and for evaluating therapeutic drugs in clinical practice.

Detection approaches including immunology, chromatography, chemiluminescence, and mass spectrometry were relatively complicated, time-consuming process and high cost [16–18]. However, fluorescence imaging technology has recently gained considerable attention and found to be crucial for the early diagnosis of clinical diseases due to its various benefits, including visualizability, real-time monitoring ability, good sensitivity and easy operation [19,20]. Notably, the development of molecular imaging tools has been particularly rapidly progressed in recent years. Several fluorescent probes used to detect CES2 have been reported [21–25]. The current fluorescent probes for monitoring CES2 activity have some drawbacks, including poor selectivity, low reaction rate, short emission wavelength and low detection

* Corresponding authors.
E-mail addresses: mapinyi@jlu.edu.cn (P. Ma), qiong_wu@jlu.edu.cn (Q. Wu), songdq@jlu.edu.cn (D. Song).

https://doi.org/10.1016/j.snb.2022.133122
Received 6 September 2022; Received in revised form 16 November 2022; Accepted 4 December 2022
Available online 6 December 2022

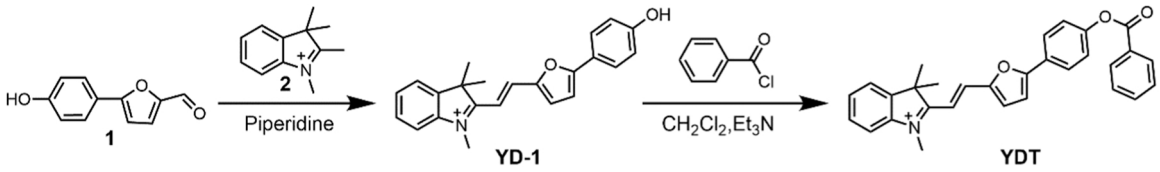

Scheme 1. Synthetic route of probe YDT.

limit [26–28]. These probes can also be easily disturbed by complex biological environments. Thus, there is an urgent need for a tool that can analyze CES2 level in vivo with ultra-high sensitivity and simplicity and can detect CES2-related diseases to improve patient survival and reduce morbidity.

Herein, a novel mitochondria-targeting near-infrared (NIR) molecular imaging tool YDT for imaging and sensing CES2 was designed and synthesized. Its properties were systematically investigated by in vitro experiments and theoretical calculations. With rapid response, easy operation, high sensitivity, good selectivity, large stokes shifts and non-invasive features and ability to minimize self-fluorescence and light scattering of tissues, YDT can allow for more accurate imaging or functional assessment.

Drug-induced liver injury (DILI) can cause liver failure or death in severe cases and may be developed into cirrhosis or liver cancer that gravely threatens human health [29,30]. Besides, acetaminophen (APAP) overdose is the most common cause of acute liver damage [30–32]. However, the complex clinical phenotypes and vague clinical symptoms of DILI cause difficulty in early diagnosis and may exacerbate the dysfunction of enzyme system. We found for the first time that CES2 can be used as a biomarker in combination with a sensitive assay to detect DILI. Due to the antioxidant properties and hepatoprotective effects of GSH, we conjecture that GSH can alleviate liver damage [33,34]. Thus, by using our designed probe YDT, we monitored the expression of CES2 in DILI and remediation model, demonstrating that the probe YDT is an effective tool for studying the pathogenesis of DILI and evaluating its pharmacological treatment effects.

Inflammation is also prevalent during the early stage of malignant disease in humans. It can reduce CES2 expression, causing the lowering of drug activation and metabolism and the increase of drug concentration, which are harmful to the body [9,35]. We also performed imaging analysis of CES2 expression during the inflammatory process. Above all, developing a molecular imaging tool that can monitor CES2 during the early diagnosis of diseases is a desirable approach for drug development and clinical practice.

2. Experimental section

2.1. Materials and instruments

Related equipment and materials used in this study are described in the Supplementary material.

2.2. Synthesis

The synthetic route of probe YDT is given in Scheme 1. Compound 1 and 2 were synthesized according to the method in the previously literature [36,37].

Synthesis of YD-1 and YDT were shown in the Supplementary material.

2.3. General procedure for CES2 detection

YDT was dissolved in dried DMSO to prepare a 1 mM stock solution. CES2 dissolved in sterilized water was diluted to 5 μg/mL and used to prepare test samples. Initially, YDT (3 μL, 1 mM) was added into a 2 mL centrifuge tube containing 10 mM phosphate buffer (PBS, pH 7.4) and used for in vitro CES2 detection. After CES2 solution at different concentrations was added, the mixture was incubated in a shaker incubator at 37 ℃ for 10 min to activate the reactions. The reaction volume was 300 μL, and the reaction comprised probe (containing 1% DMSO), enzyme, and PBS solution. The mixture was transferred to a quartz cuvette and then subjected to UV-Vis absorption and fluorescence measurements. For comparison, a control group without CES2 was also prepared and analyzed by the same methods. The excitation slit and emission slit were set at 5 nm and 2.5 nm, respectively (λ_{ex} = 498 nm, λ_{em} = 660 nm, PMT = 700 V).

3. Results and discussion

3.1. Design and synthesis of chemosensor

In this work, the NIR chemosensor YDT consists of two components: a fluorophore YD-1 and a specific CES2-recognition group, benzoyloxy.

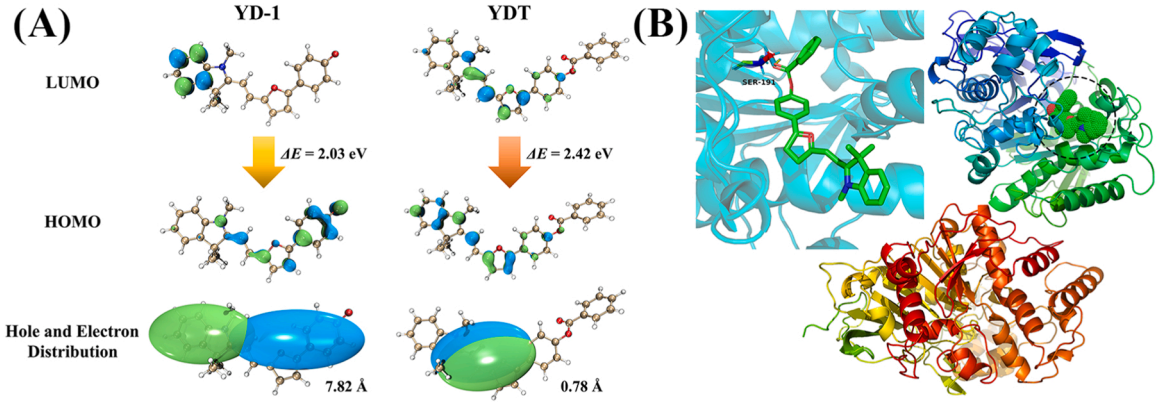

Fig. 1. (A) The frontier molecular orbitals and energy level transition of YD-1 and YDT. Space representation of hole and electron distributions for $S_1 \rightarrow S_0$ excitation. Green and blue isosurfaces correspond to electron and hole distributions, respectively. (B) Simulation of the interactions between YDT and CES2.

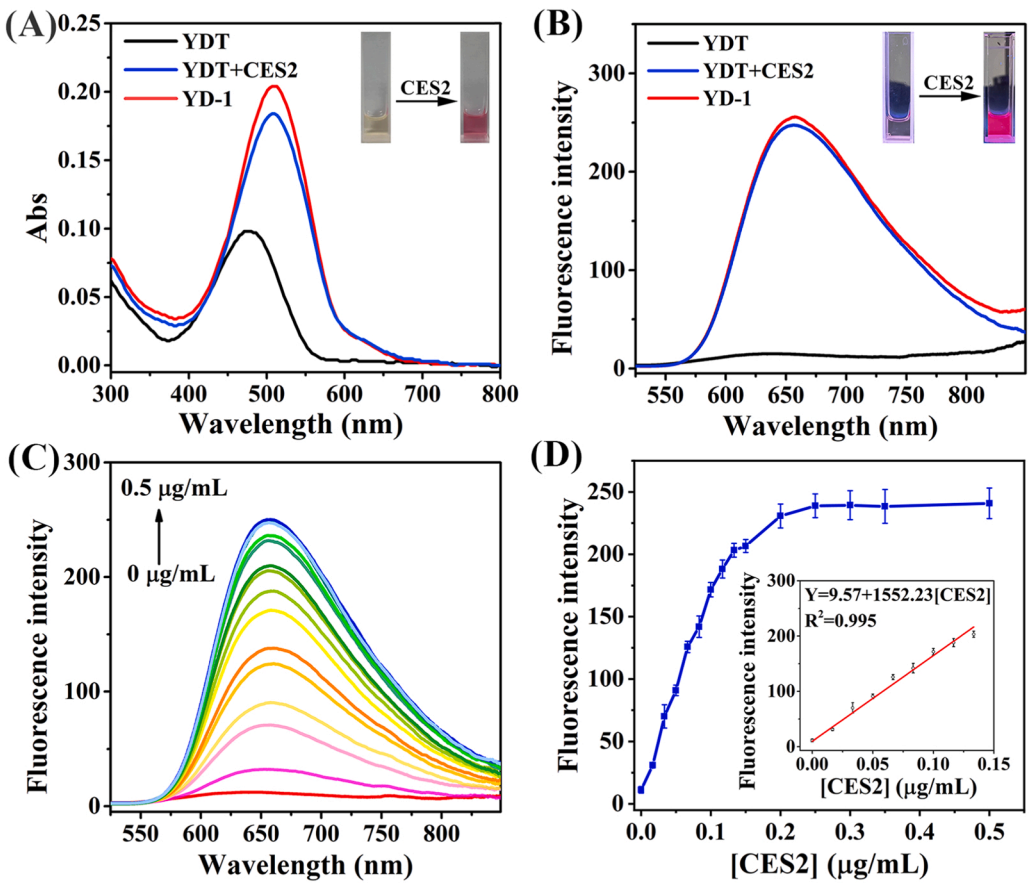

Fig. 2. (A) UV-Vis absorption and (B) fluorescence spectra of YDT (10 μM), YDT in the presence of CES2 (0.5 μg/mL), and YD-1 (10 μM) in PBS (10 mM, pH 7.4) measured at 37 °C for 10 min. The inset shows the color and fluorescence changes of the solution under natural daylight or a 365-nm UV lamp. (C) Fluorescence spectra of YDT (10 μM) upon the addition of CES2 at different concentrations (0 –0.5 μg/mL). (D) Linear relationship between fluorescence intensity and CES2 concentration. Data are expressed as the mean ± SD (n = 3). $\lambda_{ex}/_{em}$ = 498/660 nm.

The typical D-π-A structure of YDT exhibits weak fluorescence because the benzoyloxy group is bound to the hydroxyl group of the fluorophore YD-1, reducing the electron donor capacity and inhibiting the intramolecular charge transfer (ICT) process. This triggering group can be selectively recognized by CES2 and cleaved in an enzyme-catalyzed reaction, resulting in the release of fluorophore YD-1 that generates fluorescence as the ICT progress resumes. In order to further verify the hydrolysis of CES2, we analyzed the reaction substance by HR-MS (Fig. S7) and HPLC (Fig. S8). The HR-MS spectrum of YDT displayed a single peak at *m/z* 448.1908 and a retention time t_1 = 4.25 min. After incubating with CES2 (0.1 μg/mL) for 10 min, a new peak appeared at *m/z* 344.1232, and the probe produced YD-1 appeared at a new retention time t_2 = 3.74 min

TDDFT theoretical calculation (Fig. 1A) further showed that the $S_1 \rightarrow S_0$ transition of YDT and YD-1 occurred at the LOMO→HOMO energy levels with the energy level differences of 2.42 and 2.03 eV, respectively. Compared with YDT, YD-1 has a stronger push-pull electronic effect. The charge transfer distance (D_{CT}) of YDT and YD-1 was 7.82 and 0.78 Å, respectively, demonstrating that the effect of ICT caused by the first excited orbital of YD-1 is far more significant than that of ICT caused by YDT. For this reason, YD-1 was able to exhibit a stronger fluorescence emission.

Molecular docking simulation showed that YDT binds to CES2 through a hydrogen bond formed between a carbonyl group of YDT and an amino acid SER-191 (Fig. 1B). YDT better fitted with the cavity of CES2 with the binding energy of − 10.0 kcal/mol. This indicates that YDT can strongly bind to CES2.

3.2. Spectral response of YDT to CES2

The spectroscopic study of the chemosensor YDT in the presence of CES2 was investigated in vitro. The spectral properties including changes in absorption and fluorescence were evaluated. As can be seen in Fig. 2A, the characteristic UV absorption peak of the chemosensor YDT was concentrated at 480 nm. After incubating CES2 with YDT, the intensity of the absorption peak at 480 nm gradually decreased, and a new red-shifted peak appeared at 510 nm, which coincides with the maximum absorption wavelength of YD-1 fluorophore. The solution color observed by the naked eye instantly changed from orange to pink, which is the same as the color of the fluorophore. YDT emitted weak fluorescence. However, in response to CES2, a new fluorescence emission peak at 660 nm appeared in accordance with fluorophore YD-1 (Fig. 2B). The NIR chemosensor YDT with large stokes shift (150 nm) can effectively eliminate the interference of spectral overlap and self-absorption, thus improve the signal-to-noise ratio of imaging significantly. The results proved that YDT could serve as a "naked eye" colorimetric tool and an "off-on" fluorescent chemosensor for detection of CES2 activity.

3.3. Quantitative linear response of CES2

The concentration dependency of the enzymatic reaction was performed (experimental conditions were optimized in the Supplementary material). Fig. 2C shows that the fluorescence intensity of YDT at 660 nm increased significantly with CES2 concentration, and the fluorescence intensity was enhanced by approximately 30 folds. The reaction between YDT and CES2 in the buffer system at 37 °C was completed rapidly and reached a plateau within 10 min (Fig. S9). Additionally, the inset of Fig. 2D shows a strong linear relationship between the fluorescence intensity and CES2 concentrations at 0–0.15 μg/mL. YDT had a detection limit of as low as 0.165 ng/mL. Compared with the detection limits of other CES2 detection probes (Table S1), the detection limit of YDT is the lowest. Thus it is the most sensitive CES2 probe to date, and can be employed in a wide range of applications.

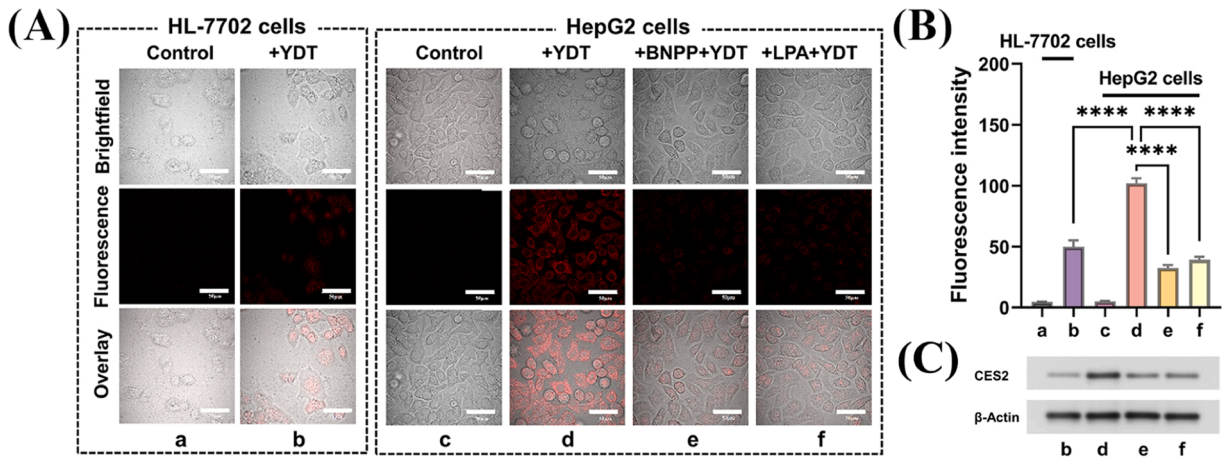

Fig. 3. (A) Confocal fluorescence images of endogenous CES2 in HL-7702 cells and HepG2 cells: (a) non-treated HL-7702 cells; (b) HL-7702 cells incubated with YDT (10 μM) for 30 min; (c) non-treated HepG2 cells; (d) HepG2 cells incubated with YDT (10 μM) for 30 min; (e) HepG2 cells treated with BNPP (1 mM) for 1 h, followed by YDT for 30 min; and (f) HepG2 cells treated with LPA (1 mM) for 1 h, followed by YDT for 30 min. Scale bar: 50 μm. (B) Fluorescence intensity of (a-f) in (A). From top to bottom: brightfield, fluorescence, and overlay images. (C) Western blot analysis for CES2 expression levels in the above corresponding cells. (****$P < 0.0001$, data analyses were performed with an independent samples test with equal variances, means ± SD, n = 7. λex = 488 nm, λem =630–690 nm).

3.4. Quantification of CES2 in HLMs and correlation studies

To further explore the practical application of YDT, we evaluated the hydrolytic activity of CES2 on the substrate probe YDT in 12 individual HLM samples. As shown in Fig. S14A, there was approximately 4.5-fold individual variation in the CES2-mediated catalytic activity of YDT hydrolysis by CES2, which is consistent with previous reports in the literature [38–40]. Furthermore, a strong correlation with high coefficient parameter ($R^2 = 0.9579$, $P < 0.0001$) was obtained between the hydrolysis rate of YDT and that of irinotecan (CPT-11, a type of anticancer agent that can be activated by CES2) (Fig. S14B). These findings strongly suggest that YDT can be used to measure the true activity of CES2 in complex biological samples with multiple human enzymes with high reliability of quantification.

3.5. Cell imaging experiments

3.5.1. Cytotoxicity test

The viability of HepG2 cells exceeded 85 % after 24 h of incubation with YDT at a concentration of up to 20 μM (Fig. S15). This indicated that the chemosensor has good biocompatibility and is suitable for use in the following bioimaging experiments.

3.5.2. Sensing endogenous CES2 in cells

The capability of YDT in imaging endogenous CES2 in living cells was investigated. As shown in Fig. 3, when YDT was incubated with HL-7702 and HepG2 cells, respectively. Compared with the control group, there emerge fluorescence in both cells. In addition, the fluorescence intensity of HepG2 cells was significantly higher than that of HL-7702 by 2 folds. This suggests that the CES2-overexpressing HepG2 cells can react with the probe with good cell permeability and release the fluorophore. Subsequently, the HepG2 cells were pretreated with inhibitor BNPP (a generic CES inhibitor) or LPA (a specific CES2 inhibitor) before being treated with YDT. As expected, the fluorescence signals were dramatically reduced, indicating that YDT can only be hydrolyzed by CES2. Western blot assay (Fig. 3C) show that HepG2 cells incubated with YDT show an increase of band signals; this means that probe YDT can selectively label CES2. However, the band signals increased slightly in

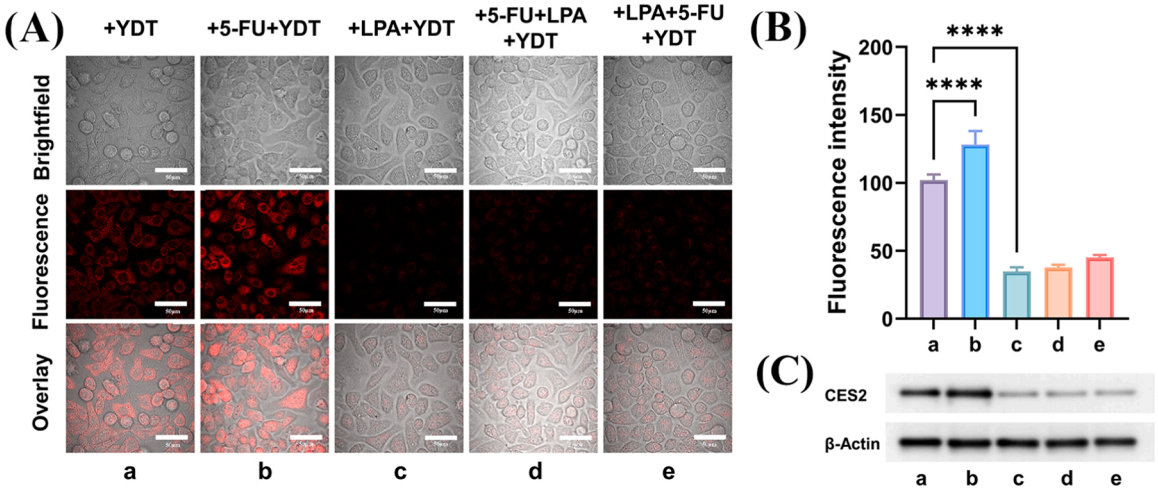

Fig. 4. (A) Dynamic monitoring of CES2 in HepG2 cells: (a) cells incubated with YDT (10 μM) for 30 min; (b) cells treated with 5-FU (1 mM) for 1 h, followed by YDT for 30 min; (c) cells treated with LPA (1 mM) for 1 h, followed by YDT (10 μM) for 30 min; (d) cells treated with 5-FU (1 mM) for 1 h, followed by LPA (1 mM) for 1 h and YDT for 30 min (e) HepG2 cells treated with LPA (1 mM) for 1 h, followed by 5-FU (1 mM) for 1 h and YDT for 30 min (B) Fluorescence intensity of (a-e) in (A). (C) Western blot analysis for CES2 expression levels in the above corresponding cells. (****$P < 0.0001$, data analyses were performed with an independent samples test with equal variances, means ± SD, n = 7. λex = 488 nm, λem = 630–690 nm).

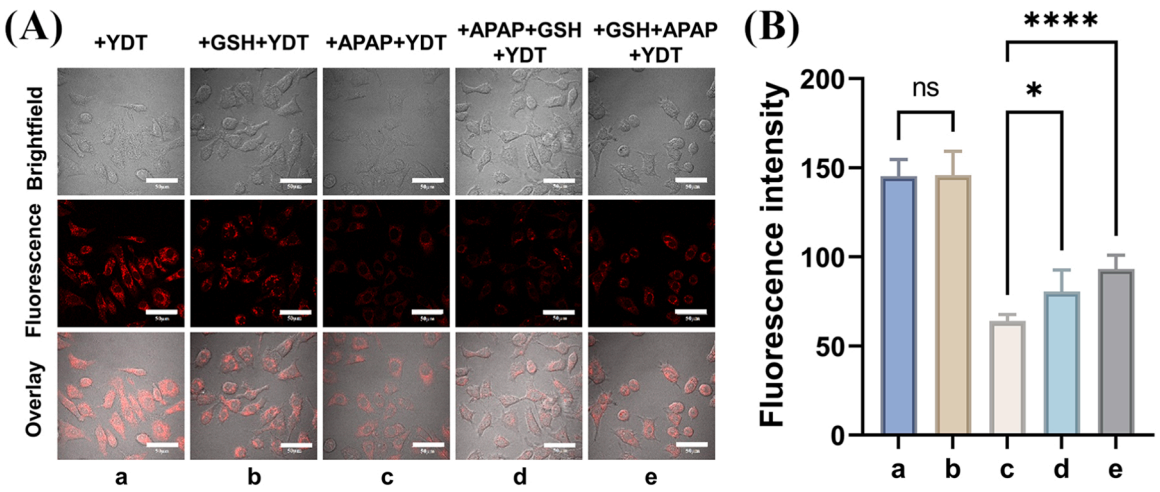

Fig. 5. (A) Fluorescent imaging of GSH-treated APAP-induced hepatotoxicity in living HepG2 cells: (a) cells were treated with YDT (10 μM) alone; (b) cells were treated with GSH (1 mM) for 8 h, followed by YDT; (c) cells were treated with APAP (1 mM) for 8 h, and then incubated with YDT; (d) cells were treated with APAP (1 mM) for 8 h, followed by GSH (1 mM) for 8 h and YDT; and (e) cells were treated with GSH (1 mM) for 8 h, followed by APAP (1 mM) for 8 h and YDT. (B) Fluorescence intensity of different treatments in (A). Scale bar: 50 μm. (ns = no significant, *P < 0.1, ****P < 0.0001, data analyses were performed with an independent samples test with equal variances, means ± SD, n = 7. λex = 488 nm, λem = 630–690 nm).

HL-7702 cells incubated with YDT. In sum, HepG2 cells contain a higher level of endogenous CES2 than HL-7702 cells, and YDT can be a useful tool for detecting CES2 activities in living cells and can distinguish cancer cells from normal cells with good selectivity.

Afterwards, we chose a commercial organelle tracker to track the subcellular organelle localization of YDT. As previously reported, YDT's indole group can target mitochondria, where CES2 is expressed. Hence, we evaluated the localization of YDT in mitochondria. In this experiment, fluorescence images and intensity profiles were carried out (Fig. S16). As expected, the red fluorescence signal of YDT and the green fluorescence signal of mitochondria-targeting dye, Mito-Tracker Green, were overlapped to a large degree with a Pearson's coefficient of 0.98. Based on the above findings, YDT can be used as a specifically mitochondria-targeting probe to determine the changes in endogenous CES2 level.

3.5.3. *Dynamic monitoring of CES2 expression in HepG2 cells*

5-FU is a vital anticancer drug due to its broad antitumor activity and synergism with other anticancer treatments [41,42]. CES2 metabolizes an anticancer prodrug CAPE to a toxic active substance 5-FU, which is a particularly important substance for the treatment of gastrointestinal cancers [43]. In addition, 5-FU is an inducer of CES2 and can increase its expression [28]. As exhibited in Fig. 4, when cells were treated with only 5-FU, the content of CES2 increased, as confirmed by the highest fluorescence intensity. When cells were treated with only inhibitor LPA, the fluorescence intensity was lowest. After CES2 expression was promoted and then the inhibitor was added, the fluorescence intensity decreased significantly, but remained slightly higher than that of only treating inhibitor. When the CES2 expression was inhibited and then promoted, the fluorescence intensity was also lower than that of the control group, but was slightly higher than the group in which the CES2 expression was promoted and then inhibited, and western blot assay results further confirm this result (Fig. 4C). The fluorescent response is required for the precise assessment of actual enzyme activity; thus, this reveals that YDT is sensitive to the change in cellular CES2 level. Monitoring the dynamic changes of CES2 under different external stimuli is beneficial to the understanding of CES2-associated physiological processes.

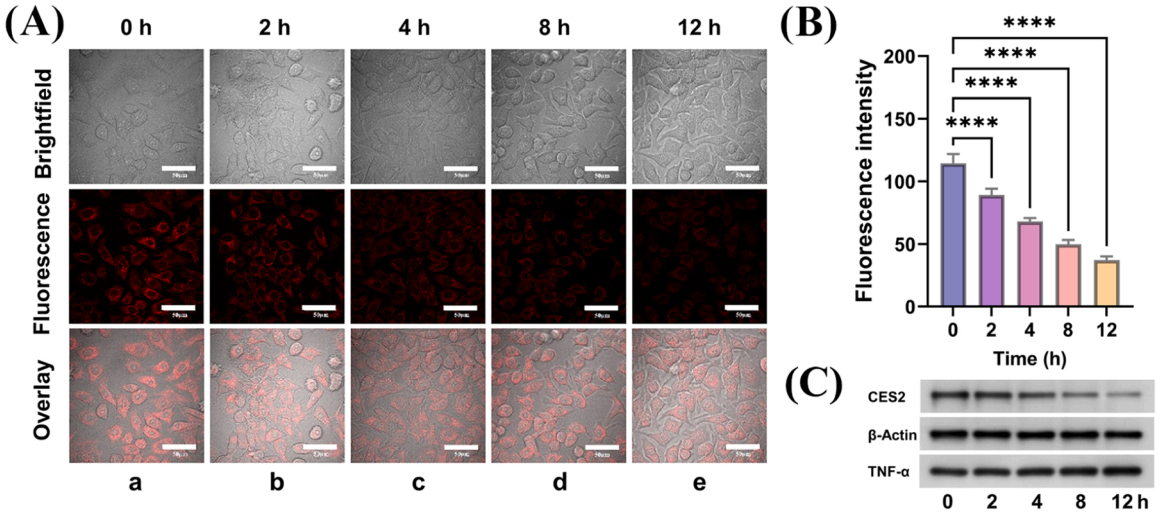

Fig. 6. (A) Time-dependent fluorescence imaging of LPS-induced inflammation in HepG2 cells. Cells were pretreated with 1 μg/mL LPS for 0, 2, 4, 8 or 12 h and then incubated with YDT (10 μM) for 30 min (B) Fluorescence intensity at different times of (A). (C) Western blot assay of CES2 in normal and inflammation cells. (****P < 0.0001, data analyses were performed with an independent samples test with equal variances, means ± SD, n = 7. λex = 488 nm, λem = 630–690 nm).

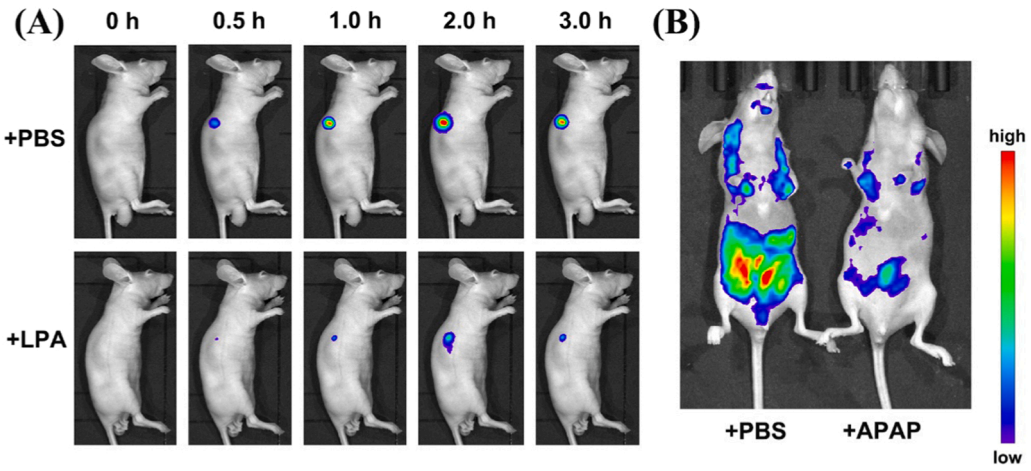

Fig. 7. (A) In situ fluorescence images of HepG2 tumor-bearing mice. Mice were intratumorally injected with 50 μL of PBS (top) and LPA (down) for 1 h and then subjected to intratumoral injection with 50 μL of YDT (200 μM) for different periods of time. (B) In vivo fluorescence images of mice intraperitoneally preinjected with PBS (left) and 300 mg/kg APAP (right) before being intravenously injected with 100 μL of YDT (200 μM).

3.5.4. Investigation of the fluctuation of CES2 in APAP-induced hepatotoxicity and remediation in cells

APAP is an important method for constructing liver injury models. According to earlier research, APAP can cause endoplasmic reticulum (ER) stress both in vivo and in vitro [44,45]. This is a deleterious condition that can contribute to liver cell death and can generate the redox imbalance that severely inhibit the functions of ER oxidoreductases. Since ER is the main site for CES2 synthesis, ER stress leads to the decrease in CES2 expression. Therefore, we speculate that APAP-induced liver injury may lead to abnormal CES2 expression. Glutathione (GSH) is a major intracellular reducing agent that protect hepatocytes from oxidative damage, as well as to protect hepatocyte membranes and promote liver detoxification and synthesis. GSH can greatly reverse or lessen the redox imbalance caused by oxidative stress and can restore the cell damage caused by liver injury to a certain extent [46]. Theoretically, using exogenous GSH supplements could aid in protecting against and healing from liver damage.

Based on these characteristics, the fluorescence response of the probe to CES2 in APAP-induced acute liver injury at different times and in remediated cells was measured. As depicted in Fig. S17, the fluorescence intensity decreased with the increase of APAP incubation time, thus predicting more severe cell damage. Statistical analysis showed that APAP could cause damage to cells after only 2 h of incubation.

When cells were incubated with GSH followed by YDT, indicating that GSH had almost no effect on the expression of CES2. However, the fluorescence intensity of cells treated with GSH before inducing liver injury or cells treated with GSH after inducing liver injury significantly increased compared with that of cells in the APAP-only group. The CES2 expression was rebounded but could not fully recover to the normal level. The results illustrated in Fig. 5 confirm our hypothesis.

Consequently, it is clinically important to establish APAP-induced cellular liver injury model and determine the changes of CES2 expression in cells by YDT. GSH can act not only as a hepatoprotective agent, but also as a detoxifying agent to remedy the damage caused by liver injury and keep CES2 within a normal level.

3.5.5. Inflammation in living cells

In pathological conditions such as inflammation and infection, the secretion of various cytokines is significantly increased, and the hydrolytic metabolism of prodrugs is reduced. Therefore, inflammation is closely related to CES2. Correspondingly, when LPS pretreated the cells, the remarkable time-dependent fluorescence signal gradually weakened to disappear in the inflammation model (Fig. 6). This reflects the down-regulation of intracellular CES2 concentration in inflammatory cells, which we clearly confirmed in western blot analysis with the classical inflammatory indicator TNF-α (gradual increase) (Fig. 6C).

These time-effect relationships manifest that the expression and activity of CES2 is reduced due to inflammation or liver injury, which has important significant pharmacological and toxicological implications. Overall, it is possible to diagnose early diseases and assess the healing effects of hepatoprotective medications on DILI by using probe and fluorescence imaging technologies.

3.6. Mouse imaging experiments

To evaluate the imaging performance of YDT in vivo, the probe was further applied to image in mouse model. As shown in Fig. 7A, before the intratumoral injection with YDT, the background fluorescence signal of the mouse was very low. After YDT were intratumorally injected in mice of the experimental group, an obvious fluorescent signal appeared at the tumor site, and the signal could sustain for 3 h. In contrast, when mice in the control group were injected with LPA, the fluorescence signal at the tumor site became significantly lower compared with that of mice in the experimental group. Therefore, it can be concluded that the fluorescence signal observed in the tumor site was caused by the enzyme activity of CES2 and YDT were capable of detecting CES2 in vivo. Furthermore, we imaged the in vivo CES2 activity in drug-induced injury mode using YDT. As shown in Fig. 7B, the fluorescence signal of mice with intraperitoneal injection of PBS and tail intravenous injection of YDT, was strong after 12 h post-injection. However, the fluorescence signal of nude mice intraperitoneally injected with 300 mg/kg APAP, followed by YDT, was distinct weakening after 12 h post-injection. This implies that CES2 was down-regulated in the drug-induced injury model. These results suggest that the probe suits for in vivo imaging of CES2 and has a significant clinical value.

4. Conclusions

In summary, the first mitochondrial-targeting NIR fluorescent chemosensor YDT was developed and used for detecting CES2 activity. According to in vitro tests, YDT could be easily hydrolyzed by CES2, resulting in notable changes of color and fluorescence spectrum. The changes were clearly distinguishable by both visual inspection and fluorescence analysis. YDT was successfully applied to detect endogenous CES2, from which the data showed that CES2 was more abundant in HepG2 cells than in normal liver cells. Moreover, this is the first report that the dynamic monitoring of CES2 activity upon the presence of different external stimuli. Both cellular and in vitro experiments

demonstrated that the "smart" imaging tool YDT has high selectivity (based on a test using 69 interferences) and high sensitivity with a detection limit of 0.165 ng/mL (the lowest among all CES2 detection probes). Remarkably, the successful imaging of CES2 in APAP-induced liver injury and its remediation using YDT suggests that detection of CES2 may serve as new, accurate monitoring measure sign of DILI in the living body. We were the first to uncover that liver injury led to a downregulation of CES2 expression, and GSH-treated liver injury led to the upregulation of CES2 expression. Besides, we also uncovered that LPS-induced inflammation caused a significant decrease of CES2 level. Therefore, YDT may have a broad range of applications from discovering novel therapeutic mechanisms and assessing therapy outcomes to early diagnosis of liver-related diseases associated with CES2.

CRediT authorship contribution statement

Jiaxin Li: Conceptualization, Investigation, Data curation, Validation and Writing – original draft preparation. **Jingrui Cao**: Data curation, Investigation, Investigation for biological experiments. **Wen Wu**: Data curation, Investigation. **Lanlan Xu**: Formal analysis and software. **Siqi Zhang**: Data curation, Investigation. **Pinyi Ma**: Conceptualization, Project administration, Data curation, Writing-review & editing and software. **Qiong Wu**: Investigation, Resources, Writing-review and software. **Daqian Song**: Project administration, Funding acquisition, Resources, Supervision.

Declaration of Competing Interest

The authors declare that they have no known competing financial interests or personal relationships that could have appeared to influence the work reported in this paper.

Data availability

Data will be made available on request.

Acknowledgments

This work was supported by the National Natural Science Foundation of China (22004046 and 22074052), the Norman Bethune Program of Jilin University (2022B21), the Natural Science Foundation of Jilin Province (YDZJ202101ZYTS024).

Appendix A. Supporting information

Supplementary data associated with this article can be found in the online version at doi:10.1016/j.snb.2022.133122.

References

[1] W.L. Yin, W.G. Yin, B.S. Huang, L.X. Wu, Neuroprotective effects of lentivirus-mediated cystathionine-beta-synthase overexpression against 6-OHDA-induced parkinson's disease rats, Neurosci. Lett. 657 (2017) 45–52.
[2] B. Lozano-Torres, J.F. Blandez, F. Sancenon, R. Martinez-Manez, Chromo-fluorogenic probes for beta-galactosidase detection, Anal. Bioanal. Chem. 413 (2021) 2361–2388.
[3] S. Casey Laizure, V. Herring, Z. Hu, K. Witbrodt, R.B. Parker, The role of human carboxylesterases in drug metabolism: have we overlooked their importance? Pharmacotherapy 33 (2013) 210–222.
[4] Z.M. Liu, L. Feng, G.B. Ge, X. Lv, J. Hou, Y.F. Cao, et al., A highly selective ratiometric fluorescent probe for in vitro monitoring and cellular imaging of human carboxylesterase 1, Biosens. Bioelectron. 57 (2014) 30–35.
[5] M.R. Redinbo, S. Bencharit, P.M. Potter, Human carboxylesterase 1: from drug metabolism to drug discovery, Biochem. Soc. T 31 (2003) 620–624.
[6] D. Wang, L. Zou, Q. Jin, J. Hou, G. Ge, L. Yang, Human carboxylesterases: a comprehensive review, Acta Pharm. Sin. B 8 (2018) 699–712.
[7] M.A. Ruby, J. Massart, D.M. Hunerdosse, M. Schonke, J.C. Correia, S.M. Louie, et al., Human carboxylesterase 2 reverses obesity-induced diacylglycerol accumulation and glucose intolerance, Cell Rep. 18 (2017) 636–646.
[8] G. Chalhoub, S. Kolleritsch, L.K. Maresch, U. Taschler, L. Pajed, A. Tilp, et al., Carboxylesterase 2 proteins are efficient diglyceride and monoglyceride lipases possibly implicated in metabolic disease, J. Lipid Res. 62 (2021), 100075.
[9] Y.L. Qi, H.R. Wang, L.L. Chen, B. Yang, Y.S. Yang, Z.X. He, et al., Multifunctional fluorescent probe for simultaneously detecting microviscosity, micropolarity, and carboxylesterases and its application in bioimaging, Anal. Chem. 94 (2022) 4594–4601.
[10] S.Y. Liu, X. Zou, Y. Guo, X. Gao, A highly sensitive and selective enzyme activated fluorescent probe for in vivo profiling of carboxylesterase 2, Anal. Chim. Acta 1221 (2022), 340126.
[11] M. Hosokawa, Structure and catalytic properties of carboxylesterase isozymes involved in metabolic activation of prodrugs, Molecules 13 (2008) 412–431.
[12] T. Satoh, M. Hosokawa, The mammalian carboxylesterases: from molecules to functions, Annu. Rev. Pharmacol. 38 (1998) 257–288.
[13] T. Imai, Human carboxylesterase isozymes: catalytic properties and rational drug design, Drug Metab. Pharmacokinet. 21 (2006) 173–185.
[14] S. Bencharit, C.C. Edwards, C.L. Morton, E.L. Howard-Williams, P. Kuhn, P. M. Potter, et al., Multisite promiscuity in the processing of endogenous substrates by human carboxylesterase 1, J. Mol. Biol. 363 (2006) 201–214.
[15] J. Lian, R. Nelson, R. Lehner, Carboxylesterases in lipid metabolism: from mouse to human, Protein Cell 9 (2018) 178–195.
[16] T. Steinkamp, F. Schweppe, B. Krebs, U. Karst, A tripod ligand as new sensitiser for the enzyme amplified lanthanide luminescence determination of esterase, Analyst 128 (2003) 29–31.
[17] M. Zhao, T. Zhang, F. Yu, L. Guo, B. Wu, E4bp4 regulates carboxylesterase 2 enzymes through repression of the nuclear receptor Rev-erbalpha in mice, Biochem. Pharmacol. 152 (2018) 293–301.
[18] M. Koitka, J. Höchel, D. Obst, A. Rottmann, H. Gieschen, H.-H. Borchert, Determination of rat serum esterase activities by an HPLC method using S-acetylthiocholine iodide and p-nitrophenyl acetate, Anal. Biochem. 381 (2008) 113–122.
[19] J.S. Sidhu, N. Kaur, N. Singh, Trends in small organic fluorescent scaffolds for detection of oxidoreductase, Biosens. Bioelectron. 191 (2021), 113441.
[20] L.M. Wysocki, L.D. Lavis, Advances in the chemistry of small molecule fluorescent probes, Curr. Opin. Chem. Biol. 15 (2011) 752–759.
[21] L. Feng, Z.M. Liu, L. Xu, X. Lv, J. Ning, J. Hou, et al., A highly selective long-wavelength fluorescent probe for the detection of human carboxylesterase 2 and its biomedical applications, Chem. Commun. 50 (2014) 14519–14522.
[22] X. Tian, F. Yan, J. Zheng, X. Cui, L. Feng, S. Li, et al., Endoplasmic reticulum targeting ratiometric fluorescent probe for carboxylesterase 2 detection in drug-induced acute liver injury, Anal. Chem. 91 (2019) 15840–15845.
[23] M.-m Zhang, P. Li, F. Hai, Y. Jia, Determination of carboxylesterase 2 by fluorescence probe to guide pancreatic adenocarcinoma profiling, Chem. Phys. Lett. 785 (2021), 139143.
[24] X.Y. Zhang, T.T. Liu, J.H. Liang, X.G. Tian, B.J. Zhang, H.L. Huang, et al., A highly selective near infrared fluorescent probe for carboxylesterase 2 and its biological applications, J. Mater. Chem. B 9 (2021) 2457–2461.
[25] K. Kailass, O. Sadovski, M. Capello, Y. Kang, J.B. Fleming, S.M. Hanash, et al., Measuring human carboxylesterase 2 activity in pancreatic cancer patient-derived xenografts using a ratiometric fluorescent chemosensor, Chem. Sci. 10 (2019) 8428–8437.
[26] S.J. Park, Y.J. Kim, J.S. Kang, I.Y. Kim, K.S. Choi, H.M. Kim, Carboxylesterase-2-selective two-photon ratiometric probe reveals decreased carboxylesterase-2 activity in breast cancer cells, Anal. Chem. 90 (2018) 9465–9471.
[27] Z.-M. Liu, L. Feng, J. Hou, X. Lv, J. Ning, G.-B. Ge, et al., A ratiometric fluorescent sensor for highly selective detection of human carboxylesterase 2 and its application in living cells, Sens. Actuators B Chem. 205 (2014) 151–157.
[28] Y. Wang, F. Yu, X. Luo, M. Li, L. Zhao, F. Yu, Visualization of carboxylesterase 2 with a near-infrared two-photon fluorescent probe and potential evaluation of its anticancer drug effects in an orthotopic colon carcinoma mice model, Chem. Commun. 56 (2020) 4412–4415.
[29] F. Bai, W. Du, X. Liu, L. Su, Z. Li, T. Chen, et al., A NO-responsive ratiometric fluorescent nanoprobe for monitoring drug-induced liver injury in the second near-infrared window, Anal. Chem. 93 (2021) 15279–15287.
[30] A. Reuben, D.G. Koch, W.M. Lee, G. Acute Liver Failure Study, Drug-induced acute liver failure: results of a U.S. multicenter, prospective study, Hepatology 52 (2010) 2065–2076.
[31] Y. Pan, M. Cao, D. You, G. Qin, Z. Liu, Research progress on the animal models of drug-induced liver injury: current status and further perspectives, Biomed. Res. Int. 2019 (2019), 1283824.
[32] D. Cheng, W. Xu, L. Yuan, X. Zhang, Investigation of drug-induced hepatotoxicity and its remediation pathway with reaction-based fluorescent probes, Anal. Chem. 89 (2017) 7693–7700.
[33] N. Wang, H. Wang, J. Zhang, X. Ji, H. Su, J. Liu, et al., Diketopyrrolopyrrole-based sensor for over-expressed peroxynitrite in drug-induced hepatotoxicity via ratiometric fluorescence imaging, Sens. Actuators B Chem. 352 (2022), 130992.
[34] C. Jing, Y. Wang, X. Song, X. Li, Y. Feng, M. Kou, et al., A dual-fluorophore and dual-site multifunctional fluorescent sensor for real-time visualization of mitochondrial ONOO-/GSH cross-talk in living cells, Sens. Actuators B Chem. 365 (2022), 131847.
[35] Y. Liu, Z. He, Y. Yang, X. Li, Z. Li, H. Ma, New fluorescent probe with recognition moiety of bipiperidinyl reveals the rise of hepatocellular carboxylesterase activity during heat shock, Biosens. Bioelectron. 211 (2022), 114392.
[36] T. Hosoya, H. Aoyama, T. Ikemoto, Y. Kihara, T. Hiramatsu, M. Endo, et al., Dantrolene analogues revisited: general synthesis and specific functions capable of

discriminating two kinds of Ca^{2+} release from sarcoplasmic reticulum of mouse skeletal muscle, Bioorgan. Med. Chem. 11 (2003) 663–673.
[37] X. Mu, Y. Lu, F. Wu, Y. Wei, H. Ma, Y. Zhao, et al., Supramolecular nanodiscs self-assembled from non-ionic heptamethine cyanine for imaging-guided cancer photothermal therapy, Adv. Mater. 32 (2020), e1906711.
[38] L. Feng, Z.M. Liu, J. Hou, X. Lv, J. Ning, G.B. Ge, et al., A highly selective fluorescent ESIPT probe for the detection of human carboxylesterase 2 and its biological applications, Biosens. Bioelectron. 65 (2015) 9–15.
[39] Q. Jin, L. Feng, D.D. Wang, Z.R. Dai, P. Wang, L.W. Zou, et al., A two-photon ratiometric fluorescent probe for imaging carboxylesterase 2 in living cells and tissues, ACS Appl. Mater. Interfaces 7 (2015) 28474–28481.
[40] Q. Jin, L. Feng, D.D. Wang, J.J. Wu, J. Hou, Z.R. Dai, et al., A highly selective near-infrared fluorescent probe for carboxylesterase 2 and its bioimaging applications in living cells and animals, Biosens. Bioelectron. 83 (2016) 193–199.
[41] K. Miura, M. Kinouchi, K. Ishida, W. Fujibuchi, T. Naitoh, H. Ogawa, et al., 5-FU metabolism in cancer and orally-administrable 5-FU drugs, Cancers 2 (2010) 1717–1730.
[42] D. Xiao, D. Yang, L. Guo, W. Lu, M. Charpentier, B. Yan, Regulation of carboxylesterase-2 expression by p53 family proteins and enhanced anti-cancer activities among 5-fluorouracil, irinotecan and doxazolidine prodrug, Br. J. Pharmacol. 168 (2013) 1989–1999.
[43] D.B. Longley, D.P. Harkin, P.G. Johnston, 5-fluorouracil: mechanisms of action and clinical strategies, Nat. Rev. Cancer 3 (2003) 330–338.
[44] H. Jaeschke, M.R. McGill, A. Ramachandran, Oxidant stress, mitochondria, and cell death mechanisms in drug-induced liver injury: lessons learned from acetaminophen hepatotoxicity, Drug Metab. Rev. 44 (2012) 88–106.
[45] W. Xie, J. Xie, R. Vince, S.S. More, Guanabenz attenuates acetaminophen-induced liver toxicity and synergizes analgesia in mice, Chem. Res. Toxicol. 33 (2020) 162–171.
[46] H. Ahmadvand, E. Babaeenezhad, M. Nasri, L. Jafaripour, R. Mohammadrezaei Khorramabadi, Glutathione ameliorates liver markers, oxidative stress and inflammatory indices in rats with renal ischemia reperfusion injury, J. Ren. Inj. Prev. 8 (2019) 91–97.

Jiaxin Li is currently a graduate student in College of Chemistry, Jilin University. Her interest is spectral analysis.

Jingrui Cao is currently a graduate student in China-Japan Union Hospital, Jilin University. His specialty is surgery and his interest is in oncology treatment.

Wen Wu is currently a graduate student in China-Japan Union Hospital, Jilin University. His specialty is surgery and his interest is in oncology treatment.

Lanlan Xu is currently a graduate student in College of Chemistry, Jilin University. Her interest is spectral analysis.

Siqi Zhang is currently a graduate student in College of Chemistry, Jilin University. Her interest is spectral analysis.

Pinyi Ma gained his doctor's degree from College of Chemistry, Jilin University in 2017 and he is an associate professor in that school. His research area is spectral analysis.

Qiong Wu gained her doctor's degree from College of Chemistry, Jilin University in 2018 and she is an associate professor in China-Japan Union Hospital of Jilin University. Her research area is spectral analysis and biosensor.

Daqian Song gained his doctor's degree from College of Chemistry, Jilin University in 2003 and he is a professor in that school. His research areas are spectral and chromatography analysis.